AGU PUBLICATIONS

Global Biogeochemical Cycles

RESEARCH ARTICLE
10.1002/2017GB005652

Key Points:
- Passive export of organic matter (OM) by subduction and mixing is an understudied component of the biological pump
- Regional cruises and season-long time series near the Antarctic Peninsula show that passive transport is likely ~50% of total OM export
- NO_3^- and particulate nitrogen measurements suggest passive transport may contribute approximately one fourth of total OM export throughout the Southern Ocean

Supporting Information:
- Supporting Information S1
- Table S1

Correspondence to:
M. R. Stukel,
mstukel@fsu.edu

Citation:
Stukel, M. R., & Ducklow, H. W. (2017). Stirring up the biological pump: Vertical mixing and carbon export in the Southern Ocean. *Global Biogeochemical Cycles*, *31*. https://doi.org/10.1002/2017GB005652

Received 19 FEB 2017
Accepted 25 AUG 2017
Accepted article online 31 AUG 2017

Stirring Up the Biological Pump: Vertical Mixing and Carbon Export in the Southern Ocean

Michael R. Stukel[1,2] and Hugh W. Ducklow[3]

[1]Department of Earth, Ocean, and Atmospheric Science, Florida State University, Tallahassee, FL, USA, [2]Center for Ocean-Atmospheric Prediction Studies, Florida State University, Tallahassee, FL, USA, [3]Lamont-Doherty Earth Observatory, Columbia University, Palisades, NY, USA

Abstract The biological carbon pump (BCP) transports organic carbon from the surface to the ocean's interior via sinking particles, vertically migrating organisms, and passive transport of organic matter by advection and diffusion. While many studies have quantified sinking particles, the magnitude of passive transport remains poorly constrained. In the Southern Ocean weak thermal stratification, strong vertical gradients in particulate organic matter, and weak vertical nitrate gradients suggest that passive transport from the euphotic zone may be particularly important. We compile data from seasonal time series at a coastal site near Palmer Station, annual regional cruises in the Western Antarctic Peninsula (WAP), cruises throughout the broader Southern Ocean, and SOCCOM (Southern Ocean Carbon and Climate Observations and Modeling) autonomous profiling floats to estimate spatial and temporal patterns in vertical gradients of nitrate, particulate nitrogen (PN), and dissolved organic carbon. Under a steady state approximation, the ratio of $\partial PN/\partial z$ to $\partial NO_3^-/\partial z$ suggests that passive transport of PN may be responsible for removing 46% (37%–58%) of the nitrate introduced into the surface ocean of the WAP (with dissolved organic matter contributing an additional 3–6%) and for 23% (19%–28%) of the BCP in the broader Southern Ocean. A simple model parameterized with in situ nitrate, PN, and primary production data suggested that passive transport was responsible for 54% of the magnitude of the BCP in the WAP. Our results highlight the potential importance of passive transport (by advection and diffusion) of organic matter in the Southern Ocean but should only be considered indicative of high passive transport (rather than conclusive evidence) due to our steady state assumptions.

Plain Language Summary The biological carbon pump (BCP) transports organic carbon and nitrogen from the surface ocean to depth, leading to net uptake of CO_2 from the atmosphere. It has long been assumed that sinking particles dominate the BCP, but our results show that in the Southern Ocean a substantial proportion of this transport occurs through vertical mixing of suspended or slowly sinking particles driven by ocean physics.

1. Introduction

The ocean's ability to absorb atmospheric CO_2 is determined by the rate at which carbon is transferred from the surface ocean to the deep ocean, where CO_2 can be sequestered for periods of centuries to millennia. This vertical carbon export is mediated by two major processes, the solubility carbon pump (SCP) and the biological carbon pump (BCP). The SCP operates when cold waters (with high CO_2 saturation) sink to depth at high latitudes, thus transporting the CO_2-rich waters to depth (Raven & Falkowski, 1999; Volk & Hoffert, 1985). The BCP is initiated by the photosynthetic action of phytoplankton that convert CO_2 into organic carbon and then relies on multiple mechanisms (gravitational flux of sinking fecal pellets, aggregates, and individual cells; active transport by vertically migrating organisms; and subduction or vertical mixing of organic matter) to transport the organic carbon vertically before it can be respired back to CO_2 (Ducklow et al., 2001; Siegel et al., 2016). While the processes governing the SCP are relatively well understood, the different mechanisms of the BCP remain poorly quantified, limiting our ability to predict alterations in the BCP with climate change. Understanding the BCP in the Southern Ocean is particularly important, since altered vertical fluxes in this region have been suggested to drive glacial-interglacial variability in global atmospheric CO_2 (Martin, 1990; Moore et al., 2000; Toggweiler & Sarmiento, 2013).

Gravitational flux of sinking particles is generally considered to be the most important component of the BCP. However, regional studies quantitatively comparing the flux of sinking particulate nitrogen (PN) to rates of

new nitrogen incorporation into the surface ecosystem consistently find a deficit of gravitational flux relative to new production (Bacon et al., 1996; Maiti et al., 2009; Stukel et al., 2016), particularly in the Southern Ocean (Planchon et al., 2013; Stukel et al., 2015). It is thus clear that other processes are important for maintaining the balance between new and export production (Eppley & Peterson, 1979). Vertical mixing (whether mediated by diapycnal mixing, isopycnal mixing, or alternating regions of subduction and obduction) may be a particularly important process for organic matter transport. The primary source of new nitrogen to support many euphotic zone ecosystems is the introduction of deep NO_3^- by advective or diffusive transport. Importantly, these mixing process that introduce NO_3^- to surface waters (driven by the positive gradient of NO_3^- with depth) must also remove particulate and dissolved organic matter (POM and DOM) from the surface ocean due to the negative gradients of POM and DOM with depth. Indeed, recent in situ results have found passive transport of POM and DOM by subduction and diffusion to be important near fronts and eddies (Omand et al., 2015; Stukel et al., 2017) and modeling studies have suggested that passive export is a globally important organic carbon transport pathway (Karleskind et al., 2011; Levy et al., 2013).

Quantifying the importance of passive transport of DOM and POM in situ is difficult, because it typically requires simultaneous quantification of organic matter spatial distributions along with vertical diffusivity and three-dimensional circulation fields. Further complicating the issue in the Southern Ocean are the multiple processes capable of inducing mixing: deep convection, the seasonal mixed-layer pump, wind-driven mixing, internal waves, waves breaking on bathymetric features, physical stirring by moving icebergs, convection mediated by subsurface melting of large icebergs, and the active movements of metazoans (Dall'Olmo et al., 2016; Dewar et al., 2006; Helly et al., 2011; Kunze et al., 2006; Polzin et al., 1997; Stephenson et al., 2011; Wunsch & Ferrari, 2004). However, a first-order estimate of the proportion of nitrogen entering the surface ocean that exits via mixing of POM or DOM can be gleaned by comparing the ratio of their vertical gradients across the base of the euphotic zone. Diffusive flux (J) can be described by Fick's first law: $J = -K_z \times \partial\Phi/\partial z$ where K_z is the vertical eddy diffusivity and $\partial\Phi/\partial z$ is the vertical gradient in concentration of the property of interest. The ratio of downward diffusive flux of PN to upward diffusive flux of NO_3^- is thus equal to $-(\partial \mathrm{PN}/\partial z)/(\partial \mathrm{NO_3}/\partial z)$. In this manuscript we use published data sets of vertical gradients of PN and NO_3^- from the Western Antarctic Peninsula and the greater Southern Ocean to derive a first-order estimate of the proportion of the BCP that is driven by vertical mixing of POM and DOM. While this is necessarily an oversimplification of the complex, temporally and spatially varying physical processes that transport POM and DOM to depth, it allows us to estimate that mixing of POM is likely responsible for between one quarter and one half of the BCP in the Southern Ocean and that mixing of DOM is likely responsible for an additional 3–6% of the BCP.

2. Materials and Methods

Data for this manuscript come from four distinct sources: (1) Seasonal sampling during the ice-free summer season at a nearshore station off Anvers Island by the Palmer Long-Term Ecological Research program (data available on Palmer LTER Datazoo website, http://pal.lternet.edu/data), (2) regional cruises for the Palmer LTER program (typically in January, data also available on Datazoo website), (3) a search of programs that had uploaded Southern Ocean POM data to the Biological and Chemical Oceanography Data Management Office (BCO-DMO, www.bco-dmo.org), and (4) SOCCOM autonomous profiling float data.

2.1. LTER Regional Cruises

The sampling scheme on regional cruises included conductivity-temperature-depth-Niskin rosette deployments on cruises from 1991 to 2012. Most cruises occurred in January, with the exception of a November cruise in 1991 (Cruise 1991–09) and an August cruise in 1993 (Cruise 1993–07). Station occupations occurred on lines that were drawn roughly orthogonally to the coast and spaced 100 km apart. Prior to 2009 across-shelf station density was ~10 km and five lines were typically occupied from Adelaide Island to Anvers Island, with each line sampled from near the coast to ~160–200 km offshore. From 2009 to 2012 across-shelf sampling intensity decreased, with typically one station per line sampled in each of the coastal, shelf break, and offshore regions, and more lines were added to the southern region of the grid. Station locations varied each year based on sea ice extent. At each station, samples were taken for dissolved inorganic nutrients, particulate organic carbon and nitrogen, and (beginning in 2003) dissolved organic carbon. Sampling depths were usually chosen based on light levels, with approximately six depths spanning the euphotic

zone (to the 1% light level) and additional samples taken deeper in the water column. For the following analyses, we analyzed only sampling depths at which paired NO_3^- and PN measurements were made. We further restricted our analyses to include only samples from the upper 150 m. We excluded all stations for which these criteria did not result in at least five sampling depths.

To estimate the relative contribution of passive export (vertical mixing + subduction) of PN to total organic nitrogen export, we computed vertical gradients of NO_3^- and PN at each station using a Type I linear regression of NO_3^- (or PN) regressed against depth, typically over the upper 150 m of the water column. For dissolved organic carbon (DOC) export we computed similar gradients using only samples that had paired DOC and NO_3^- measurements. We define depth as increasing downward, so a positive gradient implies higher concentrations at depth. In a steady state ocean in which vertical mixing is the only source of new nitrogen to the surface ocean ecosystem, the ratio of the gradient of PN (or DON) to NO_3^- would determine the relative amount of new nitrogen removed by passive export of PN (or DON). In reality the situation is more complex, but we use this simple assumption to estimate the magnitude of passive export. For the implications of a nonsteady state ocean with spatiotemporally varying vertical velocities see section 4.

2.2. Southern Ocean Data Sets

To assess the relevance of our findings to the broader Southern Ocean, we searched the BCO-DMO website for data sets in non–Western Antarctic Peninsula (WAP) regions of the Southern Ocean that had vertical profiles of NO_3^- and PN. We found six such data sets (Figure 1a): (1) Controls of Ross Sea Algal Community Structure (CORSACS) studied the determinants of phytoplankton community structure in the southern Ross Sea (e.g., Long et al., 2011). (2) U.S. Joint Global Ocean Flux Study Antarctic Environment and Southern Ocean Process Study (AESOPS) was conducted in the Ross Sea and the waters north of the Ross Sea (southwest Pacific Sector of the Southern Ocean) up to a latitude of 53°S (Smith et al., 2000). (3) The Blue Water Zone (BWZ) project addressed the supply of Fe to surface waters and its impact on phytoplankton communities in the southern Drake Passage (Hopkinson et al., 2007). (4) The Coccolithophores of the Patagonia Shelf (COPAS08) cruise addressed phytoplankton dynamics in the waters above the continental shelf east of southern Argentina (Painter et al., 2010). (5) The Southern Ocean Gas Exchange (SO GasEx) experiment measured gas exchange processes in the southwest Atlantic Sector of the Southern Ocean (Ho et al., 2011). (6) The Great Calcite Belt (CalcBelt) Project studied a wide region of the Atlantic and Indian sectors of the Southern Ocean where coccolithophores were dominant in frontal regions (Balch et al., 2016; Rosengard et al., 2015). Data from the aforementioned projects were analyzed as described above for the LTER regional cruises, with the exception that we did not require that PN and NO_3^- samples come from paired depths (since often samples were drawn from separate Niskin bottles with slightly different depths). Instead, we simply required that individual casts have a minimum of five samples each for NO_3^- and PN in the upper 150 m. This depth was chosen because it consistently encompasses the primary production zone in the Southern Ocean. Applying these criteria, there were a total of 49 paired profiles from CORSACS, 155 from AESOPS, 14 from BWZ, 73 from COPAS08, 32 from SO GasEx, and 112 from CalcBelt.

In addition to these cruise data sets, we downloaded data from Southern Ocean Carbon and Climate Observations and Modeling (SOCCOM) autonomous profiling floats (Russell et al., 2014). Among other sensors, these floats are outfitted with in situ ultraviolet spectrophotometer, fluorescence, and optical backscatter sensors for estimating nitrate, chlorophyll, and POC, respectively. Reported uncertainties in these sensors are ±0.5 μmol kg^{-1} for NO_3^- and ±35 μg C L^{-1} or ±20% (whichever is larger) for POC (Johnson et al., 2017). The downloaded data set included 1741 suitable profiles. Since PN is not reported, we assume constant Redfield stoichiometry (C:N molar ratio of 106:16) to convert POC to PN. However, in the cruise data sets, C:N ratios increased with depth suggesting that our PN vertical profiles derived from SOCCOM floats are likely an underestimate of the actual vertical gradients. While the SOCCOM floats provide greater spatiotemporal coverage and higher vertical resolution than the available cruise data, we consider them to have substantially higher uncertainty.

2.3. Seasonal Sampling and One-Dimensional Model

In addition to the regional cruises, the Palmer LTER also conducts season-long (typically early November to early April) twice-weekly sampling at Station E near Palmer Station (~200 m water depth, Figure 1b). Samples are typically drawn by Go-Flo bottle from five to seven depths for nutrient analysis, POC and PN

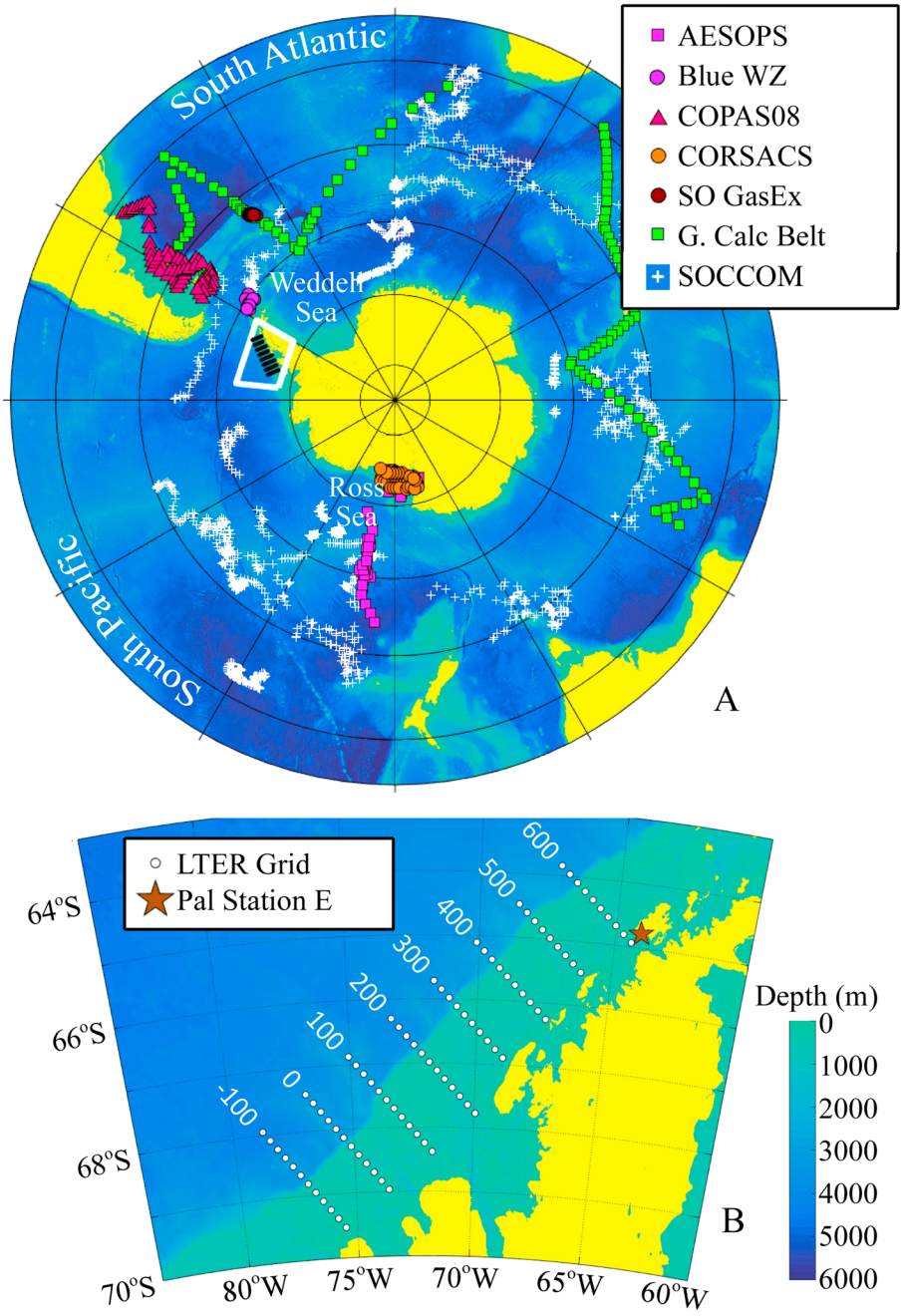

Figure 1. Study region. (a) Southern Ocean, showing the data sets included in this study. White box is the Western Antarctic Peninsula highlighted in Figure 1b. (b) Western Antarctic Peninsula, showing the full LTER grid sampling stations (white circles) and the LTER full seasonal sampling station (station E, brown star).

measurements, DOC measurements (since 2002), and $H^{14}CO_3^-$ uptake (^{14}C-PP). To assess the impact of seasonal variability (of vertical nutrient supply and PN, DOC, and NO_3^- vertical gradients) on the ratio of vertical mixing flux of PN to vertical supply of NO_3^-, we used these data sets in combination with the simple model explained below.

The rate of change of euphotic zone NO_3^- in a one-dimensional system (or a three-dimensional system with negligible horizontal gradients in NO_3^-) with minimal upwelling/downwelling can be modeled as a simple function dependent on NO_3^- assimilation by bacteria and phytoplankton, bacterial nitrification, and the resupply of NO_3^- by vertical mixing:

$$\frac{\partial NO_3^-(t)}{\partial t} = -\text{NitrateUptake}(t) + \text{Nitrification}(t) + \frac{\partial NO_3^-(t)}{\partial z}\kappa_z(t)$$

where $\kappa_z(t)$ is the temporally varying vertical eddy diffusivity which we calculate from a 1-D N-cycle model, as explained below, and NO_3^- uptake and nitrification are both vertically integrated over the euphotic zone. Thus, we can calculate $\kappa_z(t)$ from the twice-weekly vertical profiles of NO_3^- taken near Palmer Station if we can also estimate NO_3^- uptake and nitrification rates. NO_3^- uptake was measured twice weekly at Palmer Station from November 2012 to April 2013 (Stukel et al., 2015) but is not a consistent measurement made by the LTER program. However, NO_3^- uptake rates can be estimated from the twice-weekly primary production measurements, if the *f* ratio (ratio of new:total phytoplankton production, following Dugdale & Goering, 1967) can be estimated.

The *f* ratios in the Southern Ocean are highly variable. Stukel et al. (2015) estimated an average seasonal *f* ratio of 40%, though the *f* ratio varied from 22% to ~100%. Further south, near Adelaide Island, Weston et al. (2013) measured a seasonal average of 80%. Other studies have found average *f* ratios of 44% in the Amundsen Sea (Kim et al., 2015), 23% south of Tasmania (Cavagna et al., 2011), 20–49% in a region spanning the subtropical zone to the Antarctic zone in the Atlantic Sector (Joubert et al., 2011), and 22% in a diatom bloom in the Antarctic Polar Front (Brzezinski et al., 2003). In a review of Southern Ocean N Cycling, Cochlan (2008) suggests that *f* ratios may be higher in the coastal and continental shelf zone than in the permanently open ocean zone. Nevertheless it is clear that the f ratio varies substantially depending on location, season, phytoplankton community, and trace metal availability. Thus while we choose to begin with the 40% *f* ratio measured by Stukel et al. (2015) at our study site, we also test the impact of *f* ratios varying from 20 to 70% on our results. We furthermore begin by assuming that shallow water nitrification is negligible but assess the impact of varying rates of nitrification on our results.

While primary production measurements combined with assumed *f* ratios give us information about the likely NO_3^- uptake rates, NO_3^- drawdown provides an additional information source. Specifically, when NO_3^- drawdown is high (as frequently occurs early in the season), it often corresponds to high *f* ratios. We thus used this additional information source to calculate NO_3^- uptake with the following equation:

$$\text{NitrateUptake}(t) = \max\left({}^{14}\text{CPP}(t) \times R_{N:C} \times f, \text{NitrateDrawdown}(t)\right)$$

where ^{14}CPP is measured primary production and $R_{N:C}$ is the Redfield stoichiometric ratio of N:C in phytoplankton (16:106 mol:mol). Thus, we allow NO_3^- uptake to exceed our chosen *f* ratio when NO_3^- drawdown (i.e., $-\partial NO_3/\partial t$) is high.

Vertical flux of particulate organic nitrogen (PON) due to vertical mixing (PON_{export}) can be calculated from vertical gradients in PON and the vertical diffusivity gradient:

$$PON_{export}(t) = \frac{-\partial PON(t)}{\partial z}\kappa_z(t)$$

This simple conceptualization of a one-dimensional system assumes that NO_3^- supply to the euphotic zone (= NitrateUptake − Nitrification − $\partial NO_3/\partial z$) occurs through vertical mixing. However, such supply is only possible if the vertical NO_3^- gradient is positive. During periods of low stratification (common during the early and later periods of the season), surface NO_3^- concentrations are often similar to deep NO_3^- concentrations. Thus, at times (whether due to measurement inaccuracy or nutrient addition to shallow waters) the vertical NO_3^- gradient can become negative, which would lead to negative values of K_z (which is physically impossible). To avoid this issue, we set a minimum value for $\partial NO_3/\partial z$ of 0.02 μmol NO_3^- L^{-1} m^{-1}, which equates to a 1.0 μmol L^{-1} difference between the surface and the base of a 50 m euphotic zone.

2.4. Uncertainty Analysis

Throughout the manuscript, we will present the ratio of the arithmetic mean of the PN vertical gradient to the arithmetic mean of the NO_3^- vertical gradient (which reflects the proportion of upwelled NO_3^- lost as passive transport of PN averaged across the data set under the assumption of steady state) and the median of the ratios of the vertical gradient of PN to the vertical gradient of NO_3^- (which reflects the proportion of upwelled NO_3^- lost as passive transport of PN at a typical location within the data set). Since the distribution of vertical gradients was not normal, we used Monte Carlo error analysis (sampling with

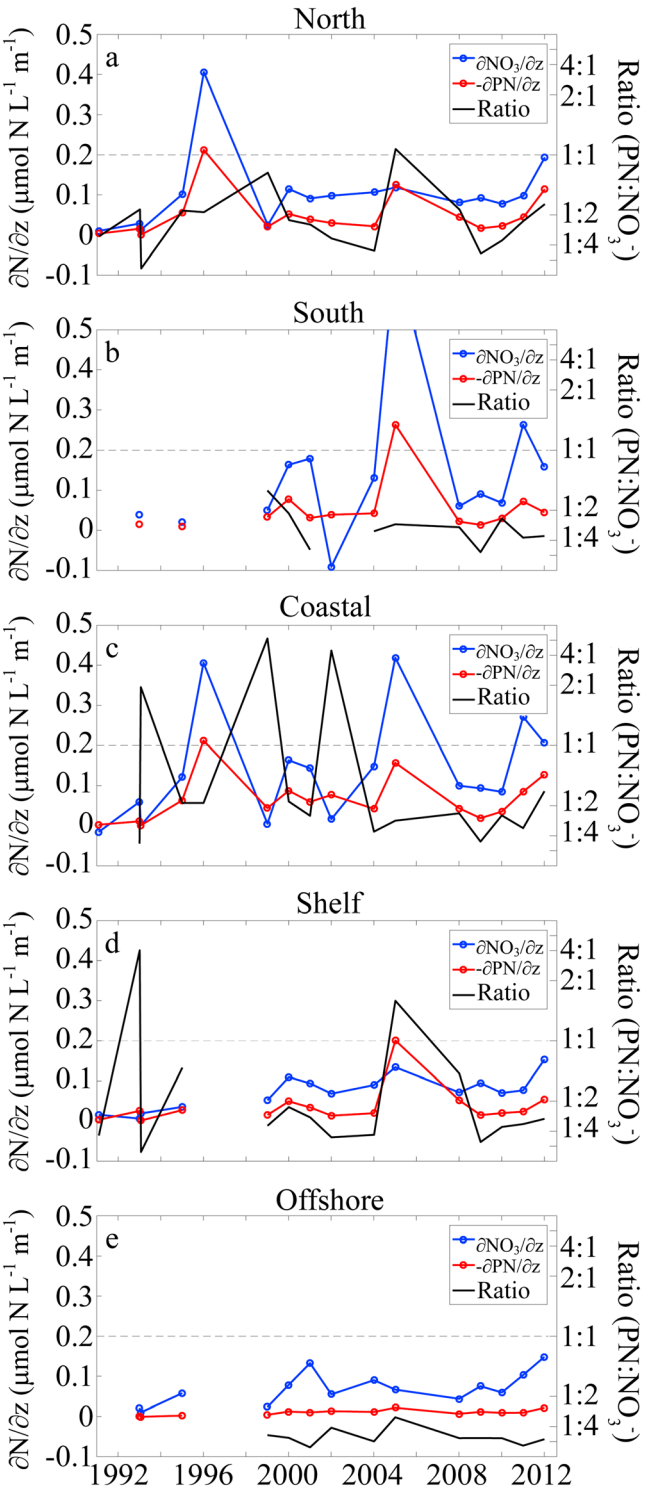

Figure 2. Cruise average vertical gradients of NO_3^- (blue), particulate nitrogen (red), and the ratio of the particulate nitrogen gradient to the NO_3^- gradient (black, only shown when both are positive, note non-linear scale) for the (a) northern, (b) southern, (c) coastal, (d) shelf, (e) and offshore regions of the WAP.

replacement) to determine uncertainty estimates (1,000 random samples drawn) and report asymmetric 95% confidence intervals for the mean and median.

Ideally, we would assess gradients only across the base of the euphotic zone (where NO_3^- is being introduced and PN is being removed). However, since discrete measurements on cruises had relatively low vertical resolution, we instead determined vertical gradients based on a linear regression of all samples in the upper 150 m. This decreased our results' sensitivity to any individual data samples (and associated error) and also led to an overall decrease in our estimate of the magnitude of vertical profiles. To assess this introduced bias, we compared vertical gradients across the base of the euphotic zone determined from SOCCOM floats to vertical gradients determined from subsampling the SOCCOM floats at depths corresponding to typical Palmer LTER data sets. This analysis suggested that using the discrete samples led to a small (~5%) overestimate of the role of vertical mixing in vertical N transport.

3. Results

3.1. Region-Wide Vertical Flux

To determine the importance of passive advective or diffusive transport of organic matter to the ocean's interior, we compared vertical gradients of PN and DOC to vertical gradients of NO_3^- from Palmer LTER cruises in the WAP (Figure 2 and Table 1). Across the data set, the median vertical NO_3^- gradient was 0.081 (95% confidence interval = 0.074–0.090) μmol N L^{-1} m^{-1}, which would correspond to an 8 μmol L^{-1} drop in NO_3^- from 100 m depth to the surface. The distribution was slightly skewed, however, and the arithmetic mean vertical gradient was 0.102 (0.085–0.118) μmol N L^{-1} m^{-1} (supporting information Figure S1a). The equivalent vertical PN gradient was −0.020 (−0.023 to −0.018) μmol N L^{-1} m^{-1}, implying an increase of 2 μmol N L^{-1} from 100 m depth to the surface, with an arithmetic mean of −0.046 (−0.058 to −0.037). The long-tail of the PN gradient highlights the frequency of bloom conditions when surface PN concentrations are much higher than the median (supporting information Figure S1b). The absolute value of the ratio of the arithmetic mean of the PN gradient to the arithmetic mean of the NO_3^- gradient reflects the proportion of total vertical NO_3^- resupply to the surface waters that would be balanced by vertical mixing of PN out of the euphotic zone if we assumed that vertical eddy diffusivity was constant across the WAP (and that diffusion was the dominant process introducing NO_3^- into the euphotic zone). This PN:NO_3^- gradient ratio equaled −0.46 (−0.58 to −0.37), suggesting that PN mixing may be responsible for 46% of the total nitrogen flux out of the euphotic zone. However, the median of the ratio of PN gradient to NO_3^- gradient was weaker (−0.27 (−0.30 to −0.24)), suggesting that at most stations PN mixing would be only one quarter of total nitrogen export. Vertical gradients of PN and NO_3^- were correlated (Pearson's correlation coefficient $\rho = -0.405$, $p < <0.001$). This indicates that high drawdown of NO_3^- was paired with high biomass accumulation of PN. However, the slope of the line was much shallower than would be expected from a 1:1 correspondence (supporting information Figure S2), indicating that PN accumulation does not perfectly balance NO_3^- drawdown (i.e., some N is lost to gravitational flux, accumulation in higher trophic levels, or conversion to DON).

Table 1
Mean (Median) Vertical Gradients and Ratio of Gradients

	$\partial NO_3/\partial z$ (μmol N L^{-1} m^{-1})	$\partial PN/\partial z$ (μmol N L^{-1} m^{-1})	$\partial POC/\partial z$ (μmol C L^{-1} m^{-1})	$\frac{\partial PN/\partial z}{\partial NO_3/\partial z}$ (mol:mol)	$\partial DOC/\partial z$ (μmol C L^{-1} m^{-1})	$\frac{\partial DOC/\partial z}{\partial NO_3/\partial z}$ (mol C:mol N)
Western Antarctic Peninsula	0.102 (0.081)	−0.046 (−0.020)	−0.28 (−0.11)	−0.46 (−0.27)	−0.052 (−0.053)	−0.44 (−0.44)
Northern Region	0.087 (0.077)	−0.043 (−0.018)	−0.24 (−0.10)	−0.49 (−0.26)	−0.048 (−0.048)	−0.45 (−0.46)
Southern Region	0.153 (0.103)	−0.059 (−0.026)	−0.43 (−0.16)	−0.39 (−0.30)	−0.060 (−0.058)	−0.44 (−0.43)
Coastal Region	0.152 (0.112)	−0.071 (−0.038)	−0.45 (−0.22)	−0.47 (−0.36)	−0.049 (−0.054)	−0.37 (−0.39)
Shelf Region	0.071 (0.067)	−0.039 (−0.018)	−0.22 (−0.10)	−0.55 (−0.27)	−0.054 (−0.050)	−0.49 (−0.49)
Offshore Region	0.064 (0.062)	−0.009 (−0.008)	−0.05 (−0.04)	−0.14 (−0.13)	0.099 (−0.053)	−0.54 (−0.53)
Station E Time Series	0.070 (0.060)	−0.047 (−0.033)	−0.31 (−0.22)	−0.67 (−0.33)	−0.076 (−0.061)	−0.53 (−0.43)
SO (Excluding WAP)	0.080 (0.069)	−0.018 (−0.009)	−0.11 (−0.06)	−0.23 (−0.19)	-	-
AESOPS	0.058 (0.034)	−0.018 (−0.007)	−0.11 (−0.04)	−0.31 (−0.29)	-	-
CORSACS	0.138 (0.121)	−0.031 (−0.024)	−0.18 (−0.14)	−0.23 (−0.23)	-	-
BWZ	0.052 (0.046)	−0.007 (−0.003)	−0.04 (−0.01)	−0.13 (−0.08)	-	-
SO GasEx	0.132 (0.136)	−0.007 (−0.008)	−0.04 (−0.05)	−0.06 (−0.06)	-	-
COPAS	0.100 (0.087)	−0.028 (−0.017)	−0.18 (−0.10)	−0.28 (−0.21)	-	-
Great Calcite Belt	0.060 (0.047)	−0.011 (−0.007)	−0.06 (−0.04)	−0.18 (−0.15)	-	-
SOCCOM Floats	0.042 (0.026)	-	−0.05 (−0.01)	−0.19 (−0.08)[a]	-	-
Spring	0.026 (0.014)	-	−0.04 (−0.02)	−0.21 (−0.16)[a]	-	-
Summer	0.084 (0.064)	-	−0.17 (−0.05)	−0.31 (−0.15)[a]	-	-
Fall	0.040 (0.028)	-	−0.02 (−0.01)	−0.07 (−0.04)[a]	-	-
Winter	0.024 (0.008)	-	−0.01 (0.00)	−0.04 (−0.02)[a]	-	-

Note. Vertical gradients are typically calculated over the upper 150 m, except for SOCCOM float data for which they are calculated only across the deep euphotic zone.
[a]For SOCCOM floats, PN estimates are not available so we assumed a constant 106:16 mol:mol C:N ratio.

The median vertical gradient of DOC was −0.053 (−0.058 to −0.047) μmol C L^{-1} m^{-1}, with a nearly identical arithmetic mean of −0.052 (−0.059 to −0.045) μmol C L^{-1} m^{-1} (Table 1 and Figures S1 and S5). If we assume a Redfield ratio of 106:16 C:N for DOM, the ratio of arithmetic mean DON gradient to arithmetic mean NO_3^- was −0.067 (−0.076 to −0.058), suggesting that 6.7% of introduced NO_3^- may be transported out of the euphotic zone as vertically mixed DON. However, if we assume the 14.9:1 mol:mol DOC:DON measured by Carlson et al. (2000) in the Ross Sea or the 11.4:1 mol:mol ratio measured in the offshore region of the WAP by Sabine et al. (2011), this value drops to −0.030 (3.0% of introduced NO_3^-) or −0.039 (3.9% of introduced NO_3^-), respectively. It is thus clear that vertical mixing of DOM is a minor, though not negligible, component of carbon and nitrogen export.

Vertical gradients of NO_3^-, PN, and DOC showed distinct spatial patterns (supporting information Figures S3–S5). To investigate these patterns in more detail, we split the grid into either two north-south regions (stations north of line 200 or south of and including line 200) or three onshore-offshore regions (coastal, shelf, and offshore, Table 1). We then took each annual cruise's average vertical gradients within each of these regions (Figure 2). It should be noted that due to logistical constraints and variable sea ice conditions, the sampled stations varied each year. Prior to 2009 there was very little sampling south of the 200 line. Nevertheless, distinct spatial patterns are evident when comparing these regions. In the northern portion of the region, NO_3^- and PN ratios were relatively uniform over time (mean for all profiles was 0.087 (0.077–0.099) and −0.043 (−0.056 to −0.033) μmol N L^{-1} m^{-1}, respectively) and the PN: NO_3^- gradient ratios typically varied between 0.25 and 1 (mean of −0.49 (−0.62 to −0.42)). In the southern region vertical gradients were more variable, with much of the variability driven by changes in the strength of the spring bloom near Marguerite Bay at the time of the cruise. Despite this variability, the mean ratio of gradients (−0.39 (−0.66 to −0.27)) was similar to that in the north. Compared to the relative similarity when comparing the northern and southern portions of the LTER grid, there were substantial differences when the stations were grouped based on distance from shore. In the coastal region, gradients were high and variable. Maximum cruise-average vertical gradients reached 0.21 and 0.42 μmol N L^{-1} m^{-1} for PN and NO_3^-, respectively, while mean values were 0.071 (0.055–0.088) and 0.15 (0.11–0.19) μmol N L^{-1} m^{-1}. The mean PN:NO_3^- gradient ratio was −0.47 (−0.61 to −0.39). Moving farther from shore, the magnitude of the gradients decreased but the ratio of gradients remained similar (mean of 0.55 (0.37–0.55) in the shelf-break region). In the

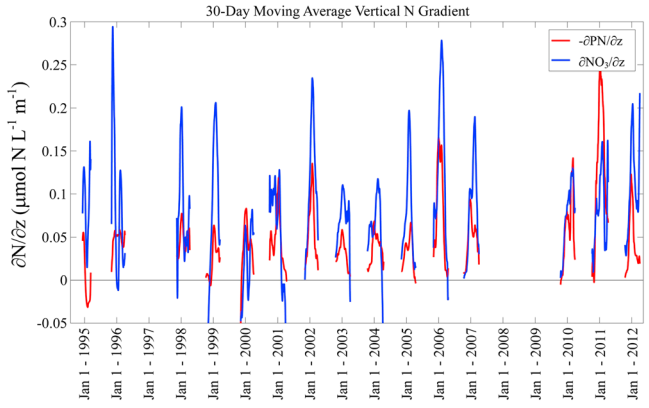

Figure 3. Vertical gradient of particulate nitrogen (red) and NO_3^- (blue) at Station E near Palmer Station (Anvers Island).

offshore region, the vertical gradients were weaker still, particularly for PN, leading to a lower ratio of 0.14 (0.12–0.17). Taken together, these results clearly show that biomass accumulation and NO_3^- drawdown were highest near the coast where large phytoplankton blooms are common, and that it is also within these coastal regions that vertical mixing of PN is most important as an export process.

3.2. Seasonal Patterns of Flux Near Palmer Station

To assess the importance of seasonal variability in vertical mixing on carbon and nitrogen fluxes, we used a twice-weekly time series of vertical profiles of NO_3^-, PN, DOC, and ^{14}CPP from LTER Station E in 200 m water depth near Palmer Station. Data were available for the ice-free summer seasons (typically November–March) from 1994 to 2012, with gaps during the 1996–1997, 2007–2008, and 2008–2009 field seasons (DOC data are only available from the 2003–2004 season to the 2011–2012 season). Thirty day moving average vertical gradients showed predictable patterns (Figure 3). During the early season (November to early December) vertical gradients were typically weak, with high surface NO_3^- and low surface PN concentrations. During the spring-summer bloom, NO_3^- was typically drawn down to 10–20 μmol L^{-1} in surface waters and PN increased to 5–10 μmol L^{-1}. Peak 30 day average vertical NO_3^- gradients ranged from 0.1–0.3 μmol N L^{-1} m^{-1}. Peak PN gradients varied from 0.05–0.25 μmol N L^{-1} m^{-1} but were typically on the low end of that range. Across the data set, the mean ratio of vertical PN gradient to vertical NO_3^- gradient was −0.67 (−0.98 to −0.48) and the median was −0.33 (−0.41 to −0.27). From 2003 to 2012, the mean ratio of vertical DOC gradient to vertical NO_3^- gradient was −0.53 (−0.78 to −0.28) mol C:mol N and median was −0.43 (−0.83 to −0.16).

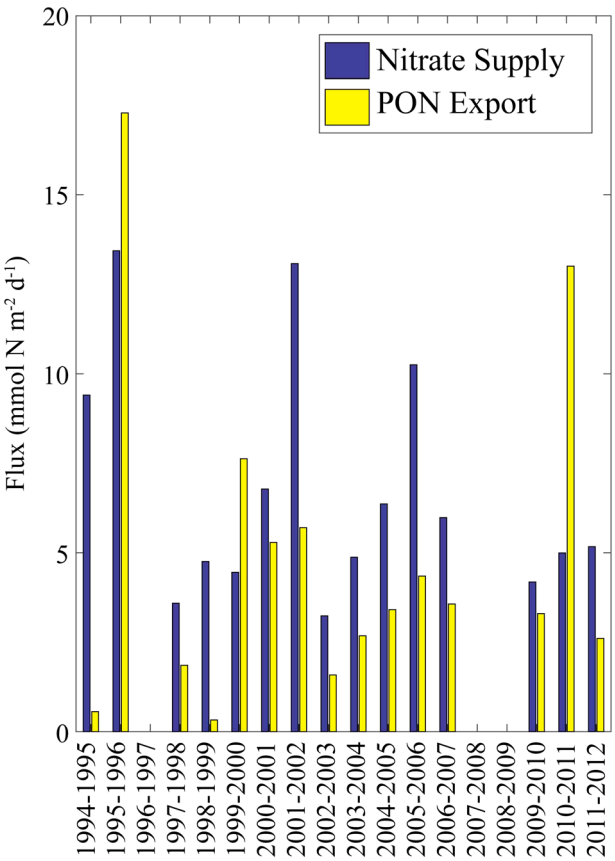

Figure 4. Season-long averages of NO_3^- supply to the euphotic zone and particulate nitrogen export due to vertical mixing at station E near Palmer Station.

While the ratio of vertical gradients can give us an estimate of the relative proportion of introduced NO_3^- that is lost to depth as passively mixed PN at a particular time and place, the mean and median of such values can be biased indicators of seasonal average rates if there is temporal variability in N diffusion. Hence, we used ^{14}CPP measurements with a nitrogen budget model to estimate temporally varying vertical diffusivity coefficients (K_z) and used these values to compute absolute NO_3^- supply and PN export rates. Assuming an f ratio of 0.4, the median of our calculated K_z near the base of the euphotic zone was 6.2×10^{-4} m^2 s^{-1}. Across the 18 year time series ice-free season median K_z ranged from 3.0×10^{-4} m^2 s^{-1} to 2.2×10^{-3} m^2 s^{-1}. These values are reasonable given previous physical model-derived estimates of K_z in the WAP that include a multiannual average of 8.5×10^{-5} m^2 s^{-1} estimated for the entire shelf region by Martinson et al. (Martinson et al., 2008) and an average of 7.7×10^{-4} m^2 s^{-1} at pycnocline depths in the Marguerite Bay region estimated by Klinck et al. (2004), along with the realization that K_z increases substantially from the pycnocline to the mixed layer.

Seasonal averages of NO_3^- flux into the euphotic zone ranged from 3.2–13.4 mmol N m^{-2} d^{-1} (average across time series of 4.9 mmol N m^{-2} d^{-1}) and seasonal fluxes of PN vertically mixed out of the euphotic zone ranged from 0.3–17.3 mmol N m^{-2} d^{-1} (average across time series of 6.7 mmol N m^{-2} d^{-1}, Figure 4). The ratio of total PN export to NO_3^- supply was thus 0.73, which was greater than the mean or median ratios of vertical gradients (−0.67 or −0.33, respectively). However, these ratios agreed favorably with the median ratio of PN export to NO_3^- supply across all seasons (0.54). The higher value for the ratio of total PN export to NO_3^- supply was driven by a few seasons (1995–1996, 1999–2000, and

2010–2011) when NO_3^- supply was relatively high, but PN export was greater than NO_3^- supply. This unlikely pattern was driven by brief periods when high NO_3^- supply was paired with a weak vertical NO_3^- gradient, leading to very high calculated values of K_z. We thus suggest that the median of the seasons (0.54) is more likely to reflect the average ratio of PN export by vertical mixing to NO_3^- supply.

To assess the impact of assuming different *f* ratios or shallow water nitrification rates on the above calculations, we repeated the calculations while varying the *f* ratio from 0.2–0.8 and varying the proportion of phytoplankton NO_3^- uptake supported by nitrification from 0 to 60%. Varying the *f* ratio (while holding nitrification rates at 0) had relatively little impact on our results. At an *f* ratio of 0.2 the median seasonal average ratio of PON export to NO_3^- supply was 0.52. At an *f* ratio of 0.8 it was 0.55. Varying the nitrification rate had a greater impact on our results, although the impact depended on the chosen *f* ratio. At our assumed *f* ratio of 0.4, the ratio of PON export to NO_3^- supply increased from 0.54 to 0.78 when nitrification was increased from 0% to 60% of NO_3^- uptake. However, if an *f* ratio of 0.8 was assumed, this value decreased from 0.55 to 0.49 when the nitrification rate was increased.

3.3. Southern Ocean Vertical Gradients

To determine if the strong vertical gradients of particulate nitrogen that we found in the WAP were a regional phenomenon or representative of the greater Southern Ocean (SO), we compiled results from other regions of the SO. Across the cruise data sets, we found broadly similar spatial patterns to those found in the WAP. Specifically, vertical gradients were typically stronger in coastal regions than in open sea areas, and the ratio of vertical PN gradient to vertical NO_3^- gradient was higher in coastal regions (Figure 5). However, the ratio of gradients was lower than that found in the WAP (mean across all the data sets was −0.23 (−0.28 to −0.19), median was −0.19 (−0.22 to −0.17)), suggesting that in the regions covered by these studies vertical mixing of PN may be responsible for approximately one fifth to one quarter of total nitrogen export.

This single value obscures substantial variability in the data sets, however (Table 1). In the AESOPS study in the Ross Sea and Pacific sector of the Antarctic Circumpolar Current the mean ratio was −0.31 (−0.36 to −0.26) but vertical gradients and the ratio of gradients generally weakened toward the north. The CORSACS study found similarly strong gradients in the Ross Sea and a mean ratio of gradients of −0.23 (−0.26 to −0.20). In the Drake Passage north of the WAP, the BWZ study measured relatively weak gradients and a mean ratio of gradients of −0.13 (−0.21 to −0.06). The SO GasEx study further to the north and east had a strong vertical NO_3^- gradient, but a weaker PN gradient, yielding a low ratio of −0.06 (−0.07 to −0.04). Further west, on the Patagonian Shelf, the COPAS study measured moderate vertical gradients with a mean ratio of −0.28 (−0.51 to −0.10). The Great Calcite Belt project sampled a broad spatial region in the northern portion of the Southern Ocean (one cruise from South America to South Africa and another from South Africa to Australia, both transiting from 35 to 60°S) and had relatively weak vertical gradients and a mean ratio of gradients (−0.18 (−0.21 to −0.14)) slightly lower than the average of the data sets. Disentangling the various seasonal, spatial, and interannual signals that lead to the variability in vertical gradients found in these studies is beyond the scope of this manuscript. Nevertheless, we find it encouraging that the mean and median ratios of these data sets (−0.23 and −0.19, respectively) were not too dissimilar from those measured in the more extensive WAP data set (−0.46 and −0.27, respectively). The agreement between these data sets and the WAP data set is even clearer when we consider the similar patterns of increasing PN vertical gradients in coastal regions and the fact that the WAP data set contained a higher proportion of coastal stations than the data sets downloaded from BCO-DMO.

When using the data from SOCCOM autonomous floats, the increased vertical resolution of the sensor measurements allowed us to consider the vertical gradient across only the deep euphotic zone (which we define herein as ranging from the chl max to the depth at which chl reaches 10% of its maximum). These depths more accurately capture the region where vertical mixing introduces NO_3^- to and removes PN from the surface ocean. The ratio of the means of PN vertical gradient to NO_3^- vertical gradient suggested that vertical mixing of PN may be responsible for 19% (15%–24%) of the biological pump (though as noted previously, this is likely an underestimate because the C:N molar ratio that we assumed for SOCCOM floats (6.625) is greater than the ratio of POC:PON vertical gradients found in either the WAP (6.0) or greater Southern Ocean cruise data set (6.1)). The SOCCOM floats also allowed us to assess temporal variability in vertical

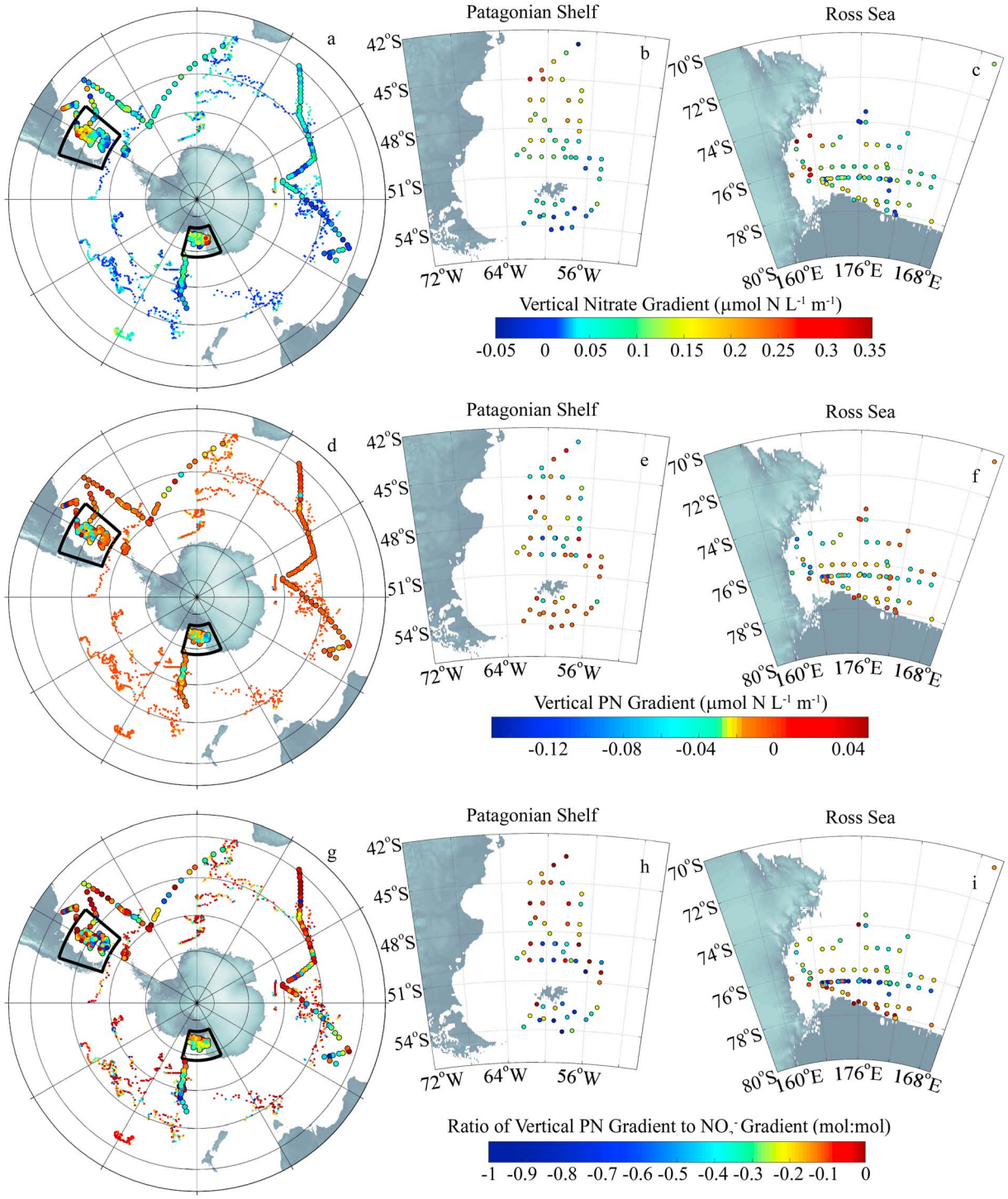

Figure 5. (a–c) Vertical NO_3^- gradients, (d–f) vertical particulate nitrogen gradients, (g–i) and the ratio of the vertical PN gradient to the vertical NO_3^- gradient in the Southern Ocean (Figures 5a, 5d, and 5g), Patagonian Shelf (Figures 5b, 5e, and 5h), and Ross Sea (Figures 5c, 5f, and 5i).

gradients, with ratios of mean gradients peaking in the summer at −0.31 (−0.41 to −0.23) and decreasing in the winter to −0.04 (−0.05 to −0.02) (Table 1). This agrees with our previous findings that the ratio of gradients was greatest during high biomass periods and suggests that definitively quantifying the importance of vertical mixing in the biological pump will require assessing covariance in temporal patterns of vertical mixing, PN, and nitrate.

4. Discussion

4.1. Vertical Particulate Nitrogen Fluxes in the Western Antarctic Peninsula

The WAP is a nutrient-rich (though sometimes iron-limited) region with high summertime new production (Bode et al., 2002; Stukel et al., 2015; Weston et al., 2013) and large standing stocks of krill and salps, which would both be expected to produce rapidly sinking fecal pellets (Gleiber et al., 2012; Steinberg et al., 2012). Nevertheless, measurements of gravitational flux in the region have typically found low to moderate flux. A long-term conical sediment trap moored at a depth of 170 m on the continental shelf measured carbon flux equal to only 4% of surface primary productivity (Ducklow et al., 2008), although a more recent calibration study using ^{238}U-^{234}Th disequilibrium has suggested that during at least late December to early January the trap was undercollecting by a substantial fraction (Buesseler et al., 2010). A more recent study using VERTEX-style sediment traps and ^{234}Th found low export ratios in the coastal WAP (7.3% with sediment traps; 9.9% with ^{234}Th) and low to moderate export ratios throughout the LTER sampling grid (median of 5.9%, range of 2.6%–47.8%) (Stukel et al., 2015). It thus seems clear that there is a substantial imbalance between the amount of NO_3^- supplied to the euphotic ecosystem and the flux of nitrogen (and carbon) transported on sinking particles.

In this study, we compared the vertical gradients of PN and NO_3^- measured throughout the WAP on cruises spanning more than a decade. If the ocean were at steady state without any horizontal gradients in properties, vertical mixing (whether by isopycnal diffusion, diapycnal diffusion, or linked upwelling and downwelling cells) would transport PN out of the surface ocean as it introduces NO_3^- to surface waters, and the ratio of PN export to NO_3^- input would be determined by the ratio of the aforementioned vertical gradients. However, as we have shown, the WAP has strong seasonality and horizontal gradients in both the onshore-offshore and north-south directions. In the following section, we will discuss the impact of this spatiotemporal variability in regional physics and ecology on our estimates of vertical PN flux, first in terms of temporal variability and then with regard to spatial variability.

The WAP (and much of the Southern Ocean) has a distinct seasonal progression of water column stratification and biological production. Cold winter surface temperatures drive deep convective mixing, effectively homogenizing the surface layer, introducing abundant NO_3^- to surface waters, and (in combination with low surface irradiance) limiting phytoplankton production. As temperatures warm in the spring/summer, the water column stratifies allowing phytoplankton blooms, NO_3^- drawdown, and PN accumulation in surface waters (Ducklow et al., 2013; Saba et al., 2014). Seasonal blooms can often be categorized as either persistent summer blooms (December–March) or briefer spring blooms (November–December), with this interannual variability tied to sea ice and atmospheric dynamics (Kim et al., 2016). Early blooms are often succeeded by periods with lower PN concentrations and a replenishment of NO_3^- in surface waters that can lead to a secondary bloom later in the season. Given these patterns of bloom progression, determining seasonal variability in mixing is clearly crucial to understanding patterns of PN passive transport. Typically, oceanographers have focused on the importance of winter deep convective mixing on transport of CO_2 to the deep ocean (i.e., the solubility pump). If deep convective mixing is the only process considered for surface ocean export as well, it would follow that only winter season vertical gradients of PN and NO_3^- are important to consider. However, this hypothesis is refuted by our measurements made near Palmer Station (Anvers Island). These twice-weekly measurements clearly show that NO_3^- replenishment (at least in coastal regions) is a continual process, not one that occurs only before the start of the phytoplankton growth season. It is possible that some of this resupply results from nitrification in surface waters, and indeed nitrification has been found to be quantitatively important in some regions of the Southern Ocean (Dehairs et al., 2015; Fripiat et al., 2015). However, we found that surface NO_3^- concentrations often increase quite rapidly, suggesting physical supply. Furthermore, these NO_3^- inputs often coincide with decreases in surface PN, as would be expected if vertical mixing was the dominant mechanism. Based on our analyses of the time series, we concluded that vertical mixing was not dominated by periods with relatively weak PN vertical gradients and strong NO_3^- gradients. Instead, our analysis found that over half of the new production near Palmer Station was removed from the euphotic zone by vertical mixing. We note, however, that this analysis assumed no horizontal variability in PN or NO_3^-. We will address this assumption presently.

In this manuscript we use the generic term vertical mixing to encompass all processes (except large-scale Ekman upwelling) that serve to introduce deep water into the surface ocean. Vertical mixing thus includes diapycnal mixing, isopycnal mixing, convective mixing, and neighboring cells of upwelling and downwelling water on mesoscale and submesoscale. These processes can be divided into processes that diffuse N through relatively still water or processes that transport N with obducted and subducted water parcels. Regardless, when integrated over a large enough scale (e.g., over a mesoscale eddy feature), this process can be modeled using Fick's first law of diffusion, and the relative amount of PN and NO_3^- transported by these processes is simply related to the relative magnitudes of their vertical gradients. However, vertical mixing (as we have defined it) is not the only process that can introduce deep NO_3^- to the surface ocean. New production could also be supported by coastal upwelling that is paired with distant (offshore) sites of subduction. In such a scenario, the strong coastal nitrate gradients (mean of 0.15 μmol N L^{-1} m^{-1}) would introduce substantial new NO_3^-, while weak offshore PN gradients (−0.009 μmol N L^{-1} m^{-1}) would result in minor PN export rates due to subduction. However, the WAP is not a traditional coastal upwelling system with Ekman transport. Rather, the general flow along the coast is predominantly southwestward and coastal winds are more commonly consistent with downwelling than upwelling conditions (Klinck et al., 2004; Moffat et al., 2008; Savidge & Amft, 2009). Nutrient injection to surface waters of the coastal WAP seems to occur predominantly through interaction of upper circumpolar deep water with bathymetric features (Dinniman & Klinck, 2004; Martinson & McKee, 2012). There is thus little reason to assume large-scale offshore transport of POM from the coast, and we believe it is reasonable to conclude that approximately 25–50% of the new production in the WAP is exported to depth via vertical mixing processes.

4.2. Mixing and the Biological Pump in the Southern Ocean

Average annual Southern Ocean primary production has been estimated from satellite remote sensing and modeling studies to fall within the range of 2–3 Pg C yr^{-1} (Arrigo et al, 2008; Carr et al., 2006; Wang & Moore, 2012). Given the range of *f* ratios that has been measured in the Southern Ocean (20–80%, Cavagna et al., 2011; Cochlan, 2008; Weston et al., 2013) it is thus clear that the magnitude of the biological pump in the Southern Ocean is in the range of 1–2 Pg C yr^{-1}, which is a substantial portion of the global biological pump (estimates range from 5 to 13 Pg C /yr, Boyd & Trull, 2007; Henson et al., 2011; Laws et al., 2011; Siegel et al., 2014).

Nevertheless, many outstanding mechanistic questions complicate attempts to predict future changes to the biological pump and marine carbon sequestration in the Southern Ocean. For instance, Fe enrichment clearly stimulates phytoplankton production and net community production in many sectors of the Southern Ocean (Coale et al., 2004; de Baar et al., 2005; Maldonado et al., 2001), yet the evidence for enhanced carbon export from these blooms remains equivocal (Buesseler et al., 2005; Nodder et al., 2001; Pollard et al., 2009; Smetacek et al., 2012). Furthermore (and of particular importance for predicting changes in the regional magnitude of the biological pump), despite predictions that the *f* ratio and export efficiency should be positively correlated with primary productivity, sediment trap and ^{238}U:^{234}Th disequilibrium measurements suggest that export efficiency is inversely correlated with primary production (Maiti et al., 2013).

Our results may help to explain some of these apparent discrepancies. In coastal regions (and other productive areas) strong vertical gradients in POM suggest that vertical mixing may be responsible for half of the biological pump. The importance of sinking flux in these regions will thus be reduced, and typical in situ measurements of the biological pump that are designed to measure sinking flux (sediment traps and ^{238}U:^{234}Th) will measure a weaker than expected biological pump. This effect could be exacerbated by processes such as active vertical transport mediated by diel vertical migrants or lateral export mediated by higher trophic levels (seabirds, whales, etc.) that further decrease the fraction of the biological pump mediated by sinking particles.

While we have so far considered diapycnal diffusion, isopycnal diffusion, and convective mixing to be similar processes, it is important to remember that they are likely to have very different biogeochemical results with respect to the remineralization length scale. Persistent diapycnal or isopycnal diffusion (the "leaky ecosystem" hypothesis suggested by Stukel et al., 2015) will be associated with moderate rates of diffusion and will only support substantial flux in depth strata with a strong vertical gradient in POM. These processes will thus lead to high flux out of the euphotic zone, but rapid flux attenuation with depth and a short remineralization length scale. By contrast, deep convective mixing (likely only dominant in winter months) is a rapid process that will be associated with a longer remineralization length scale. It is instructive to compare these

remineralization length scales to those of sinking particles, which are typically assumed to decay with either an exponential or power law relationship with depth (Buesseler & Boyd, 2009; Martin et al., 1987). It is likely that persistent diffusion would lead to a much shorter remineralization length scale than sinking flux; hence, mixing-related particle flux during summer months likely leads to a shorter time scale for carbon sequestration than sinking flux. By contrast, deep convective mixing during the winter may inject POM into deep water masses (winter mixed layer depths can exceed 500 m, Sallée et al., 2013), thus leading to more efficient carbon sequestration than typical sinking flux, although the weak gradients observed with SOCCOM floats during the winter suggest that relatively little PN is transported by this process. It must always be remembered, however, that sinking and mixing are not divergent processes that act on separate classes of particles. Slowly sinking particles may be transported out of the euphotic zone by mixing and then continue to penetrate into the deep ocean through sinking, and conversely, sinking particles may exit the euphotic zone and then get transported deeper by convective mixing.

5. Conclusions

Historically, investigations of the biological pump have focused on the role of sinking particles. Our results contribute to a growing body of literature (Levy et al., 2013; Omand et al., 2015; Stukel et al., 2017) that suggests that passive transport of POM and DOM by advection and diffusion are a globally important transport mechanism. Particularly in the Southern Ocean where NO_3^- vertical gradients are weak (because surface NO_3^- is not fully drawn down), vertical POM gradients are often strong during summer blooms, and thermal stratification is relatively weak year round, we can expect that vertical mixing plays a large role in transporting particles out of the surface productive layer. Our analysis of vertical NO_3^- and PN gradients suggests that across the Southern Ocean, vertical mixing likely contributes roughly one fourth of total transport by the biological pump, but that this ratio may be closer to one half in productive coastal regions. However, our results should be considered indicative of high export due to vertical mixing, rather than conclusive proof, since (except at one coastal station) we could not take into account temporal variability in diffusion rates and vertical gradients. We recommend that future studies make use of autonomous platforms capable of providing better spatial and temporal coverage of biogeochemical parameters in conjunction with circulation models that can accommodate spatiotemporally varying advection and diffusion rates.

Acknowledgments
We are indebted to our many friends and colleagues in the Palmer LTER program (and crews of scientific vessels) who have collected data in the WAP for the past two and half decades (especially Scott Doney who made nitrate uptake measurements and Oscar Schofield who has overseen primary production measurements). We are also grateful to the investigators from other projects who have made their data publicly available through BCO-DMO (William Balch, Giacomo DiTullio, Burke Hales, B. Gregory Mitchell, and Walker Smith). The summary data for this publication can be found in Table 1. Original data are available on Palmer LTER Datazoo website (WAP) and BCO-DMO (broader Southern Ocean). Autonomous profiling float data were collected and made freely available by the Southern Ocean Carbon and Climate Observations and Modeling (SOCCOM) Project funded by National Science Foundation, Division of Polar Programs (NSF PLR-1425989), supplemented by NOAA and NASA. This work was funded by NSF Antarctic Sciences grants 1043685 and 1440435 (Palmer LTER) from the Antarctic Organisms and Ecosystems Program to H. Ducklow.

References

Arrigo, K. R., van Dijken, G. L., & Bushinsky, S. (2008). Primary production in the Southern Ocean, 1997–2006. *Journal of Geophysical Research*, *113*, C08004. https://doi.org/10.1029/2007JC004551

Bacon, M. P., Cochran, J. K., Hirschberg, D., Hammar, T. R., & Fleer, A. P. (1996). Export flux of carbon at the equator during the EqPac time-series cruises estimated from ^{234}Th measurements. *Deep-Sea Research Part II*, *43*(4–6), 1133–1153. https://doi.org/10.1016/0967-0645(96)00016-1

Balch, W. M., Bates, N. R., Lam, P. J., Twining, B. S., Rossengard, S. Z., Bowler, B. C., … Rauschenberg, S. (2016). Factors regulating the Great Calcite Belt in the Southern Ocean and its biogeochemical significance. *Global Biogeochemical Cycles*, *30*, 1124–1144. https://doi.org/10.1002/2016GB005414

Bode, A., Castro, C. G., Doval, M. D., & Varela, M. (2002). New and regenerated production and ammonium regeneration in the western Bransfield Strait region (Antarctica) during phytoplankton bloom conditions in summer. *Deep-Sea Research Part II*, *49*(4–5), 787–804. https://doi.org/10.1016/S0967-0645(01)00124-2

Boyd, P. W., & Trull, T. W. (2007). Understanding the export of biogenic particles in oceanic waters: Is there consensus? *Progress in Oceanography*, *72*(4), 276–312. https://doi.org/10.1016/j.pocean.2006.10.007

Brzezinski, M. A., Dickson, M. L., Nelson, D. M., & Sambrotto, R. (2003). Ratios of Si, C and N uptake by microplankton in the Southern Ocean. *Deep-Sea Research Part II*, *50*(3–4), 619–633. https://doi.org/10.1016/S0967-0645(02)00587-8

Buesseler, K. O., & Boyd, P. W. (2009). Shedding light on processes that control particle export and flux attenuation in the twilight zone of the open ocean. *Limnology and Oceanography*, *54*(4), 1210–1232. https://doi.org/10.4319/lo.2009.54.4.1210

Buesseler, K. O., Andrews, J. E., Pike, S. M., Charette, M. A., Goldson, L. E., Brzezinski, M. A., & Lance, V. P. (2005). Particle export during the southern ocean iron experiment (SOFeX). *Limnology and Oceanography*, *50*(1), 311–327. https://doi.org/10.4319/lo.2005.50.1.0311

Buesseler, K. O., McDonnell, A. M. P., Schofield, O. M. E., Steinberg, D. K., & Ducklow, H. W. (2010). High particle export over the continental shelf of the west Antarctic Peninsula. *Geophysical Research Letters*, *37*, L22606, doi:https://doi.org/10.1029/2010GL045448

Carlson, C. A., Hansell, D. A., Peltzer, E. T., & Smith, W. O. (2000). Stocks and dynamics of dissolved and particulate organic matter in the southern Ross Sea, Antarctica. *Deep-Sea Research Part II*, *47*(15–16), 3201–3225. https://doi.org/10.1016/S0967-0645(00)00065-5

Carr, M.-E., Friedrichs, M. A. M., Schmeltz, M., Aita, M. N., Antoine, D., Arrigo, K. R., … Yamanaka, Y. (2006). A comparison of global estimates of marine primary production from ocean color. *Deep-Sea Research Part II*, *53*(5–7), 741–770. https://doi.org/10.1016/j.dsr2.2006.01.028

Cavagna, A. J., Elskens, M., Griffiths, F. B., Fripiat, F., Jacquet, S. H. M., Westwood, K. J., & Dehairs, F. (2011). Contrasting regimes of production and potential for carbon export in the Sub-Antarctic and Polar Frontal Zones south of Tasmania. *Deep-Sea Research Part II*, *58*(21–22), 2235–2247. https://doi.org/10.1016/j.dsr2.2011.05.026

Coale, K. H., Johnson, K. S., Chavez, F. P., Buesseler, K. O., Barber, R. T., Brzezinski, M. A., … Johnson, Z. I. (2004). Southern ocean iron enrichment experiment: Carbon cycling in high- and low-Si waters. *Science*, *304*(5669), 408–414. https://doi.org/10.1126/science.1089778

Cochlan, W. P. (2008). Nitrogen uptake in the Southern Ocean. In *Nitrogen in the marine environment* (2nd ed.) (pp. 569–596). Burlington, MA: Academic Press. https://doi.org/10.1016/B978-0-12-372522-6.00012-8

Dall'Olmo, G., Dingle, J., Polimene, L., Brewin, R. J. W., & Claustre, H. (2016). Substantial energy input to the mesopelagic ecosystem from the seasonal mixed-layer pump. *Nature Geoscience*, *9*(11), 820–823.

de Baar, H. J. W., Boyd, P. W., Coale, K. H., Landry, M. R., Tsuda, A., Assmy, P., … Wong, C.-S. (2005). Synthesis of iron fertilization experiments: From the iron age in the age of enlightenment. *Journal of Geophysical Research*, *110*, C09S16. https://doi.org/10.1029/2004JC002601

Dehairs, F., Fripiat, F., Cavagna, A. J., Trull, T. W., Fernandez, C., Davies, D., … Elskens, M. (2015). Nitrogen cycling in the Southern Ocean Kerguelen Plateau area: evidence for significant surface nitrification from nitrate isotopic compositions. *Biogeosciences*, *12*(5), 1459–1482.

Dewar, W. K., Bingham, R. J., Iverson, R. L., Nowacek, D. P., Laurent, L. C. S., & Wiebe, P. H. (2006). Does the marine biosphere mix the ocean? *Journal of Marine Research*, *64*(4), 541–561.

Dinniman, M. S., & Klinck, J. M. (2004). A model study of circulation and cross-shelf exchange on the west Antarctic Peninsula continental shelf. *Deep-Sea Research Part II*, *51*(17–19), 2003–2022.

Ducklow, H. W., Steinberg, D. K., & Buesseler, K. O. (2001). Upper ocean carbon export and the biological pump. *Oceanography*, *14*(4), 50–58.

Ducklow, H. W., Erickson, M., Kelly, J., Montes-Hugo, M., Ribic, C. A., Smith, R. C., … Karl, D. M. (2008). Particle export from the upper ocean over the continental shelf of the west Antarctic Peninsula: A long-term record, 1992-2007. *Deep-Sea Research Part II*, *55*(18–19), 2118–2131.

Ducklow, H. W., Fraser, W. R., Meredith, M. P., Stammerjohn, S. E., Doney, S. C., Martinson, D. G., … Amsler, C. D. (2013). West Antarctic Peninsula: An ice-dependent coastal marine ecosystem in transition. *Oceanography*, *26*(3), 190–203.

Dugdale, R. C., & Goering, J. J. (1967). Uptake of new and regenerated forms of nitrogen in primary productivity. *Limnology and Oceanography*, *12*(2), 196–206.

Eppley, R. W., & Peterson, B. J. (1979). Particulate organic matter flux and planktonic new production in the deep ocean. *Nature*, *282*(5740), 677–680.

Fripiat, F., Elskens, M., Trull, T. W., Blain, S., Cavagna, A.-J., Fernandez, C., … Dehairs, F. (2015). Significant mixed layer nitrification in a natural iron-fertilized bloom of the Southern Ocean. *Global Biogeochemical Cycles*, *29*, 1929–1943. https://doi.org/10.1002/2014GB005051

Gleiber, M. R., Steinberg, D. K., & Ducklow, H. W. (2012). Time series of vertical flux of zooplankton fecal pellets on the continental shelf of the western Antarctic Peninsula. *Marine Ecology Progress Series*, *471*, 23–36.

Helly, J. J., Kaufmann, R. S., Stephenson, G. R., & Vernet, M. (2011). Cooling, dilution and mixing of ocean water by free-drifting icebergs in the Weddell Sea. *Deep-Sea Research Part II*, *58*(11–12), 1346–1363.

Henson, S. A., Sanders, R., Madsen, E., Morris, P. J., Le Moigne, F., & Quartly, G. D. (2011). A reduced estimate of the strength of the ocean's biological carbon pump. *Geophysical Research Letters*, *38,* L04606. https://doi.org/10.1029/2011GL046735

Ho, D. T., Sabine, C. L., Hebert, D., Ullman, D. S., Wanninkhof, R., Hamme, R. C., … Hargreaves, B. R. (2011). Southern Ocean Gas Exchange Experiment: Setting the stage. *Journal of Geophysical Research*, *116*, C00F08. https://doi.org/10.1029/2010JC006852

Hopkinson, B. M., Mitchell, G., Reynolds, R. A., Wang, H., Selph, K. E., Measures, C. I., … Barbeau, K. A. (2007). Iron limitation across chlorophyll gradients in the southern Drake Passage: Phytoplankton responses to iron addition and photosynthetic indicators of iron stress. *Limnology and Oceanography*, *52*(6), 2540–2554.

Johnson, K. S., Plant, J. N., Coletti, L. J., Jannasch, H. W., Sakamoto, C. M., Riser, S. C., … Sarmiento, J. L. (2017). Biogeochemical sensor performance in the SOCCOM profiling float array, *Journal of Geophysical Research: Oceans*, *122*, 6416–6436. https://doi.org/10.1002/2017JC012838

Joubert, W. R., Thomalla, S. J., Waldron, H. N., Lucas, M. I., Boye, M., Le Moigne, F. A. C., … Speich, S. (2011). Nitrogen uptake by phytoplankton in the Atlantic sector of the Southern Ocean during late austral summer. *Biogeosciences*, *8*(10), 2947–2959. https://doi.org/10.5194/bg-8-2947-2011

Karleskind, P., Levy, M., & Memery, L. (2011). Subduction of carbon, nitrogen, and oxygen in the northeast Atlantic. *Journal of Geophysical Research*, *116*, C02025, doi:https://doi.org/10.1029/2010JC006446

Kim, B. K., Joo, H., Song, H. J., Yang, E. J., Lee, S. H., Hahm, D., & Rhee, T. S. (2015). Large seasonal variation in phytoplankton production in the Amundsen Sea. *Polar Biology*, *38*(3), 319–331. https://doi.org/10.1007/s00300-014-1588-5

Kim, H., Doney, S. C., Iannuzzi, R. A., Meredith, M. P., Martinson, D. G., & Ducklow, H. W. (2016). Climate forcing for dynamics of dissolved inorganic nutrients at Palmer Station, Antarctica: An interdecadal (1993–2013) analysis. *Journal of Geophysical Research: Biogeosciences*, *121*, 2369–2389. https://doi.org/10.1002/2015JG003311

Klinck, J. M., Hofmann, E. E., Beardsley, R. C., Salihoglu, B., & Howard, S. (2004). Water-mass properties and circulation on the west Antarctic Peninsula Continental Shelf in Austral Fall and Winter 2001. *Deep-Sea Research Part II*, *51*(17–19), 1925–1946. https://doi.org/10.1016/j.dsr2.2004.08.001

Kunze, E., Dower, J. F., Beveridge, I., Dewey, R., & Bartlett, K. P. (2006). Observations of biologically generated turbulence in a coastal inlet. *Science*, *313*(5794), 1768–1770. https://doi.org/10.1126/science.1129378

Laws, E. A., D'Sa, E., & Naik, P. (2011). Simple equations to estimate ratios of new or export production to total production from satellite-derived estimates of sea surface temperature and primary production. *Limnology and Oceanography: Methods*, *9*, 593–601. https://doi.org/10.4319/lom.2011.9.593

Levy, M., Bopp, L., Karleskind, P., Resplandy, L., Ethe, C., & Pinsard, F. (2013). Physical pathways for carbon transfers between the surface mixed layer and the ocean interior. *Global Biogeochemical Cycles*, *27*, 1001–1012. https://doi.org/10.1002/gbc.20092

Long, M. C., Dunbar, R. B., Tortell, P. D., Smith, W. O., Mucciarone, D. A., & DiTullio, G. R. (2011). Vertical structure, seasonal drawdown, and net community production in the Ross Sea, Antarctica. *Journal of Geophysical Research*, *116*, C10029. https://doi.org/10.1029/2009JC005954

Maiti, K., Benitez-Nelson, C. R., Lomas, M. W., & Krause, J. W. (2009). Biogeochemical responses to late-winter storms in the Sargasso Sea, III—Estimates of export production using ^{234}Th:^{238}U disequilibria and sediment traps. *Deep-Sea Research Part I*, *56*(6), 875–891. https://doi.org/10.1016/j.dsr.2009.01.008

Maiti, K., Charette, M. A., Buesseler, K. O., & Kahru, M. (2013). An inverse relationship between production and export efficiency in the Southern Ocean. *Geophysical Research Letters*, *40*, 1557–1561. https://doi.org/10.1002/grl.50219

Maldonado, M. T., Boyd, P. W., LaRoche, J., Strzepek, R., Waite, A., Bowie, A. R., … Price, N. M. (2001). Iron uptake and physiological response of phytoplankton during a mesoscale Southern Ocean iron enrichment. *Limnology and Oceanography*, *46*(7), 1802–1808. https://doi.org/10.4319/lo.2001.46.7.1802/pdf

Martin, J. H. (1990). Glacial-interglacial CO^2 change: The iron hypothesis. *Paleoceanography*, *5*(1), 1–13. https://doi.org/10.1029/PA005i001p00001

Martin, J. H., Knauer, G. A., Karl, D. M., & Broenkow, W. W. (1987). Vertex: Carbon cycling in the northeast Pacific. *Deep Sea Research*, *34*(2), 267–285. https://doi.org/10.1016/0198-0149(87)90086-0

Martinson, D. G., & McKee, D. C. (2012). Transport of warm Upper Circumpolar Deep Water onto the western Antarctic Peninsula continental shelf. *Ocean Science*, *8*(4), 433–442. https://doi.org/10.5194/os-8-433-2012

Martinson, D. G., Stammerjohn, S. E., Iannuzzi, R. A., Smith, R. C., & Vernet, M. (2008). Western Antarctic Peninsula physical oceanography and spatio-temporal variability. *Deep-Sea Research Part II*, *55*(18–19), 1964–1987. https://doi.org/10.1016/j.dsr2.2008.04.038

Moffat, C., Beardsley, R. C., Owens, B., & van Lipzig, N. (2008). A first description of the Antarctic Peninsula Coastal Current. *Deep-Sea Research Part II*, *55*(3–4), 277–293. https://doi.org/10.1016/j.dsr2.2007.10.003

Moore, J. K., Abbott, M. R., Richman, J. G., & Nelson, D. M. (2000). The Southern Ocean at the last glacial maximum: A strong sink for atmospheric carbon dioxide. *Global Biogeochemical Cycles*, *14*(1), 455–475. https://doi.org/10.1029/1999GB900051

Nodder, S. D., Charette, M. A., Waite, A. M., Trull, T. W., Boyd, P. W., Zeldis, J., & Buesseler, K. O. (2001). Particle transformations and export flux during an in situ iron-stimulated algal bloom in the Southern Ocean. *Geophysical Research Letters*, *28*(12), 2409–2412. https://doi.org/10.1029/2001GL013008

Omand, M. M., D'Asaro, E. A., Lee, C. M., Perry, M. J., Briggs, N., Cetinić, I., & Mahadevan, A. (2015). Eddy-driven subduction exports particulate organic carbon from the spring bloom. *Science*, *348*(6231), 222–225. https://doi.org/10.1126/science.1260062

Painter, S. C., Poulton, A. J., Allen, J. T., Pidcock, R., & Balch, W. M. (2010). The COPAS'08 expedition to the Patagonian Shelf: Physical and environmental conditions during the 2008 coccolithophore bloom. *Continental Shelf Research*, *30*(18), 1907–1923. https://doi.org/10.1016/j.csr.2010.08.013

Planchon, F., Cavagna, A. J., Cardinal, D., Andre, L., & Dehairs, F. (2013). Late summer particulate organic carbon export and twilight zone remineralisation in the Atlantic sector of the Southern Ocean. *Biogeosciences*, *10*(2), 803–820. https://doi.org/10.5194/bg-10-803-2013

Pollard, R. T., Salter, I., Sanders, R. J., Lucas, M. I., Moore, C. M., Mills, R. A., … Zubkov, M. V. (2009). Southern Ocean deep-water carbon export enhanced by natural iron fertilization. *Nature*, *457*(7229), 577–U581. https://doi.org/10.1038/nature07716

Polzin, K., Toole, J., Ledwell, J., & Schmitt, R. (1997). Spatial variability of turbulent mixing in the abyssal ocean. *Science*, *276*(5309), 93–96. https://doi.org/10.1126/science.276.5309.93

Raven, J. A., & Falkowski, P. G. (1999). Oceanic sinks for atmospheric CO2. *Plant, Cell & Environment*, *22*(6), 741–755. https://doi.org/10.1046/j.1365-3040.1999.00419.x/pdf

Rosengard, S. Z., Lam, P. J., Balch, W. M., Auro, M. E., Pike, S., Drapeau, D., & Bowler, B. (2015). Carbon export and transfer to depth across the Southern Ocean Great Calcite Belt. *Biogeosciences*, *12*(13), 3953–3971. https://doi.org/10.5194/bg-12-3953-2015

Russell, J., Sarmiento, J., Cullen, H., Hotinski, R., Johnson, K., Riser, S., & Talley, L. (2014). The southern ocean carbon and climate observations and modeling program (SOCCOM). *Ocean Carbon Biogeochem. Newsl*, *7*, 1–5. http://web.whoi.edu/ocb/wp-content/uploads/sites/43/2016/12/OCB_NEWS_FALL14.pdf

Saba, G. K., Fraser, W. R., Saba, V. S., Iannuzzi, R. A., Coleman, K. E., Doney, S. C., … Schofield, O. M. (2014). Winter and spring controls on the summer food web of the coastal West Antarctic Peninsula. *Nature Communications*, *5*, 4318. https://doi.org/10.1038/ncomms5318

Sabine, C., Feely, R., Wanninkhof, R., Dickson, A., Millero, F., Hansell, D., … Key, R. (2011). Carbon dioxide, hydrographic, and chemical data obtained during the R/V Nathaniel B. In O. R. N. L. Carbon Dioxide Information Analysis Center (Ed.), *Palmer cruise in the Southern Ocean on CLIVAR Repeat Hydrography Section S04P (Feb. 19–Apr. 23, 2011)*. Oak Ridge, Tennessee: US Department of Energy.

Sallée, J. B., Shuckburgh, E., Bruneau, N., Meijers, A. J., Bracegirdle, T. J., & Wang, Z. (2013). Assessment of Southern Ocean mixed-layer depths in CMIP5 models: Historical bias and forcing response. *Journal of Geophysical Research: Oceans*, *118*, 1845–1862. https://doi.org/10.1002/jgrc.20157

Savidge, D. K., & Amft, J. A. (2009). Circulation on the West Antarctic Peninsula derived from 6 years of shipboard ADCP transects. *Deep-Sea Research Part I*, *56*(10), 1633–1655. https://doi.org/10.1016/j.dsr.2009.05.011

Siegel, D. A., Buesseler, K. O., Doney, S. C., Sailley, S. F., Behrenfeld, M. J., & Boyd, P. W. (2014). Global assessment of ocean carbon export by combining satellite obervations and food-web models. *Global Biogeochemical Cycles*, *28*, 181–196. https://doi.org/10.1002/2013GB004743

Siegel, D. A., Buesseler, K. O., Behrenfeld, M. J., Benitez-Nelson, C. R., Boss, E., Brzezinski, M. A., … Doney, S. C. (2016). Prediction of the export and fate of global ocean net primary production: the EXPORTS science plan. *Frontiers in Marine Science*, *3*, 22. https://doi.org/10.3389/fmars.2016.00022

Smetacek, V., Klaas, C., Strass, V. H., Assmy, P., Montresor, M., Cisewski, B., … Wolf-Gladrow, D. (2012). Deep carbon export from a Southern Ocean iron-fertilized diatom bloom. *Nature*, *487*(7407), 313–319. https://doi.org/10.1038/nature11229

Smith, W. O., Anderson, R. F., Moore, J. K., Codispoti, L. A., & Morrison, J. M. (2000). The US Southern Ocean Joint Global Ocean Flux Study: an introduction to AESOPS. *Deep-Sea Research Part II*, *47*(15–16), 3073–3093. https://doi.org/10.1016/S0967-0645(00)00059-X

Steinberg, D. K., Martinson, D. G., & Costa, D. P. (2012). Two decades of pelagic ecology of the Western Antarctic Peninsula. *Oceanography*, *25*(3), 56–67. https://doi.org/10.5670/oceanog.2012.75

Stephenson, G. R., Sprintall, J., Gille, S. T., Vernet, M., Helly, J. J., & Kaufmann, R. S. (2011). Subsurface melting of a free-floating Antarctic iceberg. *Deep-Sea Research Part II*, *58*(11–12), 1336–1345. https://doi.org/10.1016/j.dsr2.2010.11.009

Stukel, M. R., Asher, E., Coutos, N., Schofield, O., Strebel, S., Tortell, P. D., & Ducklow, H. W. (2015). The imbalance of new and export production in the Western Antarctic Peninsula, a potentially "leaky" ecosystem. *Global Biogeochemical Cycles*, *29*, 1400–1420. https://doi.org/10.1002/2015GB005211

Stukel, M. R., Benitez-Nelson, C., Décima, M., Taylor, A. G., Buchwald, C., & Landry, M. R. (2016). The biological pump in the Costa Rica Dome: An open ocean upwelling system with high new production and low export. *Journal of Plankton Research*, *38*(2), 348–365. https://doi.org/10.1093/plankt/fbv097

Stukel, M. R., Aluwihare, L. I., Barbeau, K. A., Chekalyuk, A. M., Goericke, R., Miller, A. J., … Landry, M. R. (2017). Mesoscale ocean fronts enhance carbon export due to gravitational sinking and subduction. *Proceedings of the National Academy of Sciences*, *114*(6), 1252–1257. https://doi.org/10.1073/pnas.1609435114

Toggweiler, J. R., & Sarmiento, J. L. (2013). Glacial to interglacial changes in atmospheric carbon dioxide: The critical role of ocean surface water in high latitudes. In *The Carbon Cycle and Atmospheric CO_2: Natural Variations Archean to Present* (pp. 163–184). Washington, DC: American Geophysical Union.

Volk, T., & Hoffert, M. I. (1985). Ocean carbon pumps: Analysis of relative strengths and efficiencies in ocean-driven atmospheric CO_2 changes. In E. T. Sundquist & W. S. Broeker (Eds.), *The Carbon Cycle and Atmospheric CO_2: Natural Variations Archean to Present* (pp. 99–110). Washington, DC: American Geophysical Union.

Wang, S., & Moore, J. K. (2012). Variability of primary production and air-sea CO_2 flux in the Southern Ocean. *Global Biogeochemical Cycles*, *26*, GB1008. https://doi.org/10.1029/2010GB003981

Weston, K., Jickells, T. D., Carson, D. S., Clarke, A., Meredith, M. P., Brandon, M. A., … Hendry, K. R. (2013). Primary production export flux in Marguerite Bay (Antarctic Peninsula): Linking upper water-column production to sediment trap flux. *Deep-Sea Research Part I*, *75*, 52–66. https://doi.org/10.1016/j.dsr.2013.02.001

Wunsch, C., & Ferrari, R. (2004). Vertical mixing, energy, and the general circulation of the oceans. *Annual Review of Fluid Mechanics*, *36*, 281–314. https://doi.org/10.1146/annurev.fluid.36.050802.122121